ORIGINAL ARTICLE

Variations and Statistical Probability Characteristic Analysis of Extreme Precipitation in the Hekouzhen-Longmen Region of the Yellow River, China

Suzhen Dang[1,2] · Manfei Yao[3] · Xiaoyan Liu[4] · Guotao Dong[1,2]

Abstract

Under the impact of climate change, the variation in the magnitude and frequency of extreme precipitation events has become a major issue worldwide. Based on the daily precipitation data at 9 meteorological stations and 111 precipitation stations in the Hekouzhen-Longmen region (HLR) in the middle reaches of the Yellow River Basin during 1966–2015, the spatial and temporal variations in and statistical probability characteristics of extreme precipitation were investigated. The probability distribution of extreme precipitation in the HLR was simulated with the annual maximum (AM) series and peak over threshold (POT) series by three extreme distributions, namely, generalized extreme value (GEV) distribution, generalized Pareto (GP) distribution, and gamma distribution. The parameters of the GEV, GP and gamma distributions were estimated by the L-moments method, and the best fit model was selected by the Kolmogorov-Smirnov (K-S) test. The results showed that high value area of extreme precipitation was located in the southeast part of the HLR, while the lower value area was mainly distributed in the northwestern part of the HLR and the upper reaches of the Wuding River Basin. A positive trend of annual maximum precipitation was detected at half of the stations, and the other half of the stations were found to show a negative trend from 1966 to 2015, while the changing trends of extreme precipitation at almost all of the stations were nonsignificant. From the results of the K-S test, the GEV distribution can better fit the AM series, and the GP distribution can better fit the POT series. The estimated extreme precipitation of the AM series is larger than that of the POT series with the same return period at most stations.

Keywords Extreme precipitation · Yellow River · Probability distribution · Variation

1 Introduction

The Intergovernmental Panel on Climate Change (IPCC) fifth assessment report has pointed out that global warming is intensifying, and the frequency and intensity of extreme climate events such as high temperature and heavy rainfall will increase significantly (IPCC 2013). The resulting disasters have also increased and had a very serious impact on social stability, economic development and people's lives (Mirza 2003; Santos and Fragoso 2013). As the changes in the frequency and intensity of extreme precipitation events bring great threats to natural and social systems, studies on extreme precipitation events, especially on the analysis of spatiotemporal changes and statistical characteristics of extreme precipitation events, have attracted the attention of an increasing number of scholars in the past several decades (Plummer et al. 1999; Alexander et al. 2006; Hu et al. 2015), and these studies on extreme precipitation events are of great theoretical and practical significance.

Studies have shown that extreme precipitation changes exhibit great regional variability. The frequency of extreme precipitation events is increasing in most terrestrial areas across the world (Easterling et al. 2000; Frich et al. 2002; Alexander et al. 2006; IPCC 2013), such as India, eastern Australia and

✉ Suzhen Dang
270127774@qq.com

1   Yellow River Institute of Hydraulic Research, Yellow River Conservancy Commission, Zhengzhou 450003, China

2   Key Laboratory of Soil and Water Loss Process and Control on the Loess Plateau, MWR, Yellow River Institute of Hydraulic Research, Zhengzhou 450003, China

3   School of Water Conservancy, North China University of Water Resources and Electric Power, Zhengzhou 450045, China

4   Yellow River Conservancy Commission, Zhengzhou 450003, China

Thailand (Sen Roy and Balling 2004; Fiddes et al. 2015; Limsakul and Singhruck 2016), whereas there are significant decreasing trends in extreme precipitation events in the western part of alpine Australia and some areas of western central Africa (Aguilar et al. 2009; Fiddes and Pezza 2014; Fiddes et al. 2015). In China, the results from observational studies have also shown that the changes in extreme precipitation have large variability (Zhai et al. 2005; Wang and Qian 2009; You et al. 2011; Xia et al. 2012; Du et al. 2014; Sun et al. 2016). There are increasing trends in most areas of China, such as in northeastern and southeastern China, eastern Tibetan Plateau and Xinjiang, whereas there are decreasing trends in north China and southwestern China.

Moreover, statistical models are applied to better understand the changes in extreme precipitation events. Su et al. (2009) quantified the characteristics of extreme precipitation over the Yangtze River Basin by using four probability distributions, namely, generalized extreme value (GEV) distribution, generalized Pareto (GP) distribution, general logistic (GLO), and Wakeby (WAK), and it was found that WAK can adequately describe the probability distribution of precipitation extremes. Fischer et al. (2011) fitted the precipitation extremes in the Zhujiang River Basin by GEV, GP, WAK and gamma distributions and revealed that GEV was the most reliable and robust distribution at the basin scale in the Zhujiang River Basin. Xia et al. (2012) analyzed the precipitation events in the Huaihe River Basin with three extreme distributions, i.e., GEV, GP and gamma distributions, and the results showed that annual maximum (AM) series can be better fitted by the GEV model, and peak over threshold (POT) series can be better fitted by the GP model.

The Yellow River is characterized by less water and more sand and the uncoordinated relationship between water and sediment and is known for serious water and sand disasters. Therefore, the Yellow River Basin is very sensitive and vulnerable to climate change, and the impact of climate change on its water and sediment is of particular concern. Extreme precipitation events exert considerable impacts on floods and soil erosion in the Yellow River Basin (Xia et al. 2014; Zhang et al. 2014; Wan et al. 2015; Sun et al. 2015). In this paper, we selected the region from Hekouzhen to Longmen in the middle reaches of the Yellow River Basin (hereinafter referred to as the Hekouzhen-Longmen region, HLR) as the study area. This region is one of three storm flood source areas in the middle reaches of the Yellow River (Wang 1997) and is also the main source area of sediment in the middle reaches of the Yellow River, especially coarse sediment (Hu et al. 2008). The HLR accounts for more than 90% of the Yellow River sediment input above the Sanmenxia Reservoir (Ran 2000).

Previous studies on extreme precipitation in the study area have mainly focused on the spatial and temporal variations in precipitation (Li et al. 2010; Wan et al. 2015; Gao et al. 2015; Sun et al. 2016; Wang et al. 2017). For example,

Gao et al. (2015) found that changes in precipitation extremes on the Loess Plateau during 1960–2013 were relatively small, and the number of rainy days increased on the northern Loess Plateau, but the extreme precipitation events decreased. Sun et al. (2016) analyzed the annual and decadal trends of 10 extreme precipitation indices in terms of intensity, frequency, and duration over the Loess Plateau during 1960–2013 and indicated that the changes in days of erosive rainfall, heavy rain, rainstorm, maximum 5-day precipitation, and very-wet-day and extremely wet-day precipitation were not significant. However, the comprehensive analysis of the spatiotemporal variation in and statistical characteristics of extreme precipitation is limited.

Thus, based on the observed daily precipitation data at 120 stations in the HLR during 1966–2015, the major objectives of this study were to analyze the spatial and temporal variations in extreme precipitation and to investigate the statistical characteristics of extreme precipitation using several extreme value distribution models for the simulation and prediction of precipitation extremes in the HLR. This study will definitely contribute to a better understanding of the spatiotemporal variation in and statistical characteristics of extreme precipitation and provide a scientific basis for risk management and disaster preparedness.

2 Data and Methods

2.1 Study Area

The HLR is located in the middle reaches of the Yellow River (108°02′E~112°44′E, 35°40′N~40°34′N) (Fig. 1), covering an area of 111,586 km^2 and accounting for 14.8% of the Yellow River basin area. The length of the Yellow River main stem in the study area is 723 km. There are 21 large tributaries of the Yellow River with a catchment area of more than 1000 km^2. The main terrain is the gully region of the Loess Plateau. The study area has a temperate, continental monsoon climate and belongs to arid and semiarid regions. The spatial distribution of annual precipitation of the HLR is very uneven, ranging from less than 250 mm in the northwestern part to more than 720 mm in the southwestern part of the HLR. Furthermore, there is also a very large interannual variation in annual precipitation in the HLR, which varies from 290 mm to 620 mm, mainly concentrated in July–September.

2.2 Data

In this study, daily precipitation data collected from 9 meteorological stations and 111 precipitation stations during 1966–2015 in the HLR were used to analyze the spatiotemporal variability and probability characteristics in this area. The precipitation data from the meteorological stations were provided
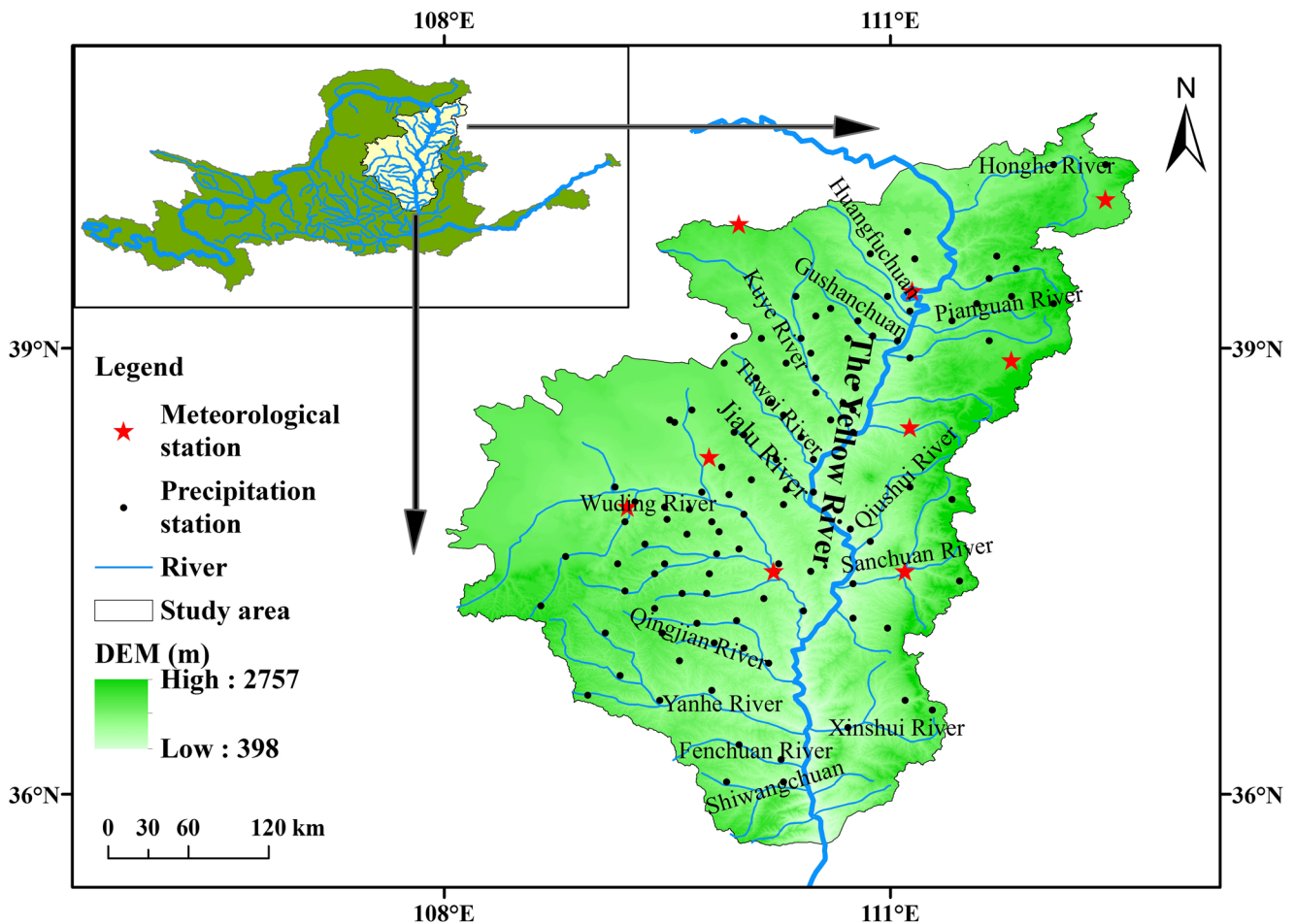
Fig. 1 Distribution map of the meteorological stations and rainfall stations in the HLR

by China Meteorological Administration (CMA), and the precipitation data from the 111 precipitation stations were from hydrological yearbook and Hydrological Bureau of Yellow River Conservancy Commission. A digital elevation model (DEM) and the locations of the meteorological stations and precipitation stations are shown in Fig. 1. A homogeneity assessment of used precipitation records in the HLR during 1966–2015 was conducted using the method proposed by Wijngaard et al. (2003), to make sure the reliability and precision of the results. The results showed that all of the data have passed the homogeneity assessment at the 0.05 significant level.

Generally, extreme precipitation refers to precipitation events that occur infrequently but with severe impacts, and it is defined as daily precipitation that exceeds a certain intensity level (such as 50 mm/d), exceeds a certain quantile (such as >95th) or reaches a certain return period (Su et al. 2008; Groisman et al. 1999; Xia et al. 2012). In this study, two kinds of extreme precipitation series are considered, the AM series and POT series. The AM series was formed by the annual maximum daily precipitation at each station from 1966 to 2015. In this study, the POT series was obtained by ranking

daily precipitation during 1966–2015 in ascending order at a station, and the 99.5th percentile of the sequence was selected as the threshold of extreme precipitation. When the daily precipitation exceeded the 99.5th percentile of all records at the station, it will be considered as extreme precipitation.

To reduce the error caused by data in establishing an optimal probability distribution model, the applicability of obtaining extreme precipitation values for the two series is discussed first. Although the precipitation information used by the AM series is limited, AM series can represent the temporal variation characteristics of extreme precipitation. There is an extreme precipitation value in each year, so the length of AM series is equal to the number of years considered. If only the AM series is considered, then the maximum daily precipitation in the dry year at a station is too low to cause extreme precipitation events, but it is selected as the extreme precipitation of this station. While in wet areas or wet years, not only the maximum precipitation event but also the second or third largest precipitation event may induce extreme precipitation events, meaning that there is more than one daily precipitation event that cause extreme precipitation events, and only one maximum can be selected, resulting in missing data. Thus, if

we only consider the AM series, then some useful information would be excluded. The sample method of the POT series greatly increases the sample size, making the best use of the information that is meant for an extreme analysis, and resolves the shortage of historical precipitation data to some extent. Although the POT series compensates for the insufficiency of the AM series, it cannot express the temporal change in extreme precipitation.

Therefore, these two methods were used to establish extreme precipitation series in this study to reduce the errors caused by the data and to improve the accuracy of establishing an optimal probability distribution model suitable for extreme precipitation in the middle reaches of the Yellow River.

An example of the AM and POT series at the Suide precipitation station is given in Fig. 2. It can be seen that the length of the POT series is greater than that of the AM series, and the extreme precipitation of the AM series in some years is even lower than the second or third largest precipitation in other years. For example, the maximum precipitation amount in 2000 is 20.9 mm, while the seventh largest precipitation amount in 2013 is 35.3 mm, and it is included in the POT series. It can also be seen that the minimum precipitation amount of the POT series is larger than some of the precipitation amounts of the AM series. It is worth noting that the average of POT series is smaller than that of the AM series for the Suide station (Fig. 2).

2.3 Methods

2.3.1 Mann-Kendall Trend Analysis Method

The Mann-Kendall (MK) trend analysis method is a nonparametric method that is recommended by the World Meteorological Organization as a standard procedure for examining trends of hydrological and meteorological time series (Mann 1945; Kendall 1955; Mitchell et al. 1966). The MK method does not require samples to follow a certain distribution and is not disturbed by a few abnormal values. It is suitable for non-normal distribution data and has been widely used (Liu and Xia 2004; Zheng et al. 2009; Saifullah et al. 2016). By assuming a normal distribution, the Mann-Kendall statistic Z can be used as a measure of a trend. $Z > 0$ indicates an increasing trend, while $Z < 0$ indicates a decreasing trend. A positive Mann-Kendall statistic Z larger than 1.96 indicates a significant increasing trend at a significance level of $P = 0.05$, while a negative Z less than −1.96 indicates a significant decreasing trend. The MK method is applied to analyze the temporal changing trend of extreme precipitation of the HLR in this study.

2.3.2 Trend-Free Pre-Whitening Mann-Kendall Test (TFPW-MK)

The TFPW-MK procedure proposed by Yue and Wang (2002) is used to detect a significant trend in a time series with significant serial correlation. Studies have demonstrated that the TFPW-MK was proved to be more effective compared with the classic MK method (Bayazit and Önöz 2007; Chen et al. 2016). TFPW-MK includes the following steps:

First, assuming the trend T_t in series X_t is linear, and removing the trend, the new series Y_t can be expressed as:

$$Y_t = X_t - T_t = X_t - \beta \cdot t \tag{1}$$

Where β is the Mann-Kendall slope, X_t is the sequential data value. β is computed as:

$$\beta = Median\left(\frac{x_j - x_i}{j - i}\right) \quad \forall i < j \tag{2}$$

Fig. 2 AM and POT series of the Suide rainfall station (the black and red solid lines represent the means of the AM and POT series, respectively, from 1966 to 2015)
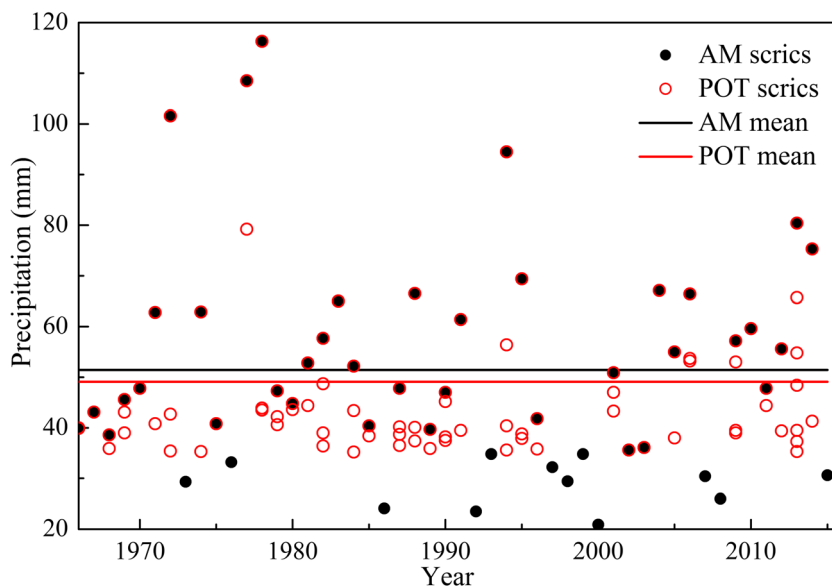
Then calculating the first-order auto-correlation coefficient (r_1) of Y_t.

$$r_1 = \frac{\sum\limits_{t=1}^{n-1} \left(x_t - \overline{x}_t\right)\left(x_{t+1} - \overline{x}_{t+1}\right)}{\sqrt{\sum\limits_{t=1}^{n-1} \left(x_t - \overline{x}_t\right)^2 \sum\limits_{t=1}^{n-1} \left(x_{t+1} - \overline{x}_{t+1}\right)^2}} \tag{3}$$

$$\frac{1 - 1.645\sqrt{n-2}}{n-1} \leq r_1(\alpha = 0.1) \leq \frac{1 + 1.645\sqrt{n-2}}{n-1} \tag{4}$$

If r_1 is within the range of formula (4), it means that the serial Y_t is independent, thus the trend test can be carried out directly with the original sequence, sequence Y_t does not need pre-whitening. Otherwise, the sequence Y_t is autocorrelated, and TFPW-MK is used to remove the autocorrelative items in the series, and a new series can be got by the following equations:

$$Y'_t = Y_t - r_1 Y_{t-1} \tag{5}$$

$$Y''_t = Y'_t + \beta t \tag{6}$$

Finally, this new sequence is adopted to test the significance of the MK method.

2.3.3 Extreme Value Distributions

The statistical characteristics of extreme precipitation were analyzed with the extreme value distributions. The GEV and GP distributions were considered in this study because they have been widely used and have shown good performance in the simulation of extreme precipitation (Kioutsioukis et al. 2010; Xia et al. 2012; She et al. 2015a, b; Zhang et al. 2018). Gamma distribution was also considered given that it has been indicated proven to be an appropriate distribution for simulating precipitation time series in China (Liang et al. 2012; Jiang et al. 2014). Therefore, the GEV, GP and gamma distributions were selected to fit the AM and POT series and further analyze the statistical probability characteristics of extreme precipitation in the HLR. The cumulative distribution function of the selected three models are given in Table 1.

2.3.4 L-Moments Method

The L-moments method, proposed by Hosking and Wallis (1997) and based on the probability weighted method, was used to estimate the parameters of the GEV, GP and gamma distributions in this study because it is convenient and more robust than the moment method. The L-moments method can directly provide estimates of the scale and shape of the probability distributions, and an in comparison to ordinary moments, it is not sensitive to the maximum and minimum values

(Hosking 1990; Hosking and Wallis 1997; Cai and Jiang 2007; Chen et al. 2014).

For a given sample $x_1, x_2, \cdots, x_n$, the order statistics of this series was denoted as $x_{1,n} \leq x_{2,n} \leq \cdots \leq x_{n,n}$. According to the definition of L-moments, the first four L-moments for any distribution can be calculated as follows (Xiong and Guo 2003; She et al. 2013):

$$\begin{cases} L_1 = \beta_0 \\ L_2 = 2\beta_1 - \beta_0 \\ L_3 = 6\beta_2 - 6\beta_1 + \beta_0 \\ L_4 = 20\beta_3 - 30\beta_2 + 12\beta_1 - \beta_0 \end{cases} \tag{7}$$

where

$$\beta_0 = \frac{1}{n}\sum_{j=1}^{n} x_{j,n}, \beta_1 = \frac{1}{n}\sum_{j=2}^{n}\frac{j-1}{n-1}x_{j,n}, \beta_2 = \frac{1}{n}\sum_{j=3}^{n}\frac{(j-1)(j-2)}{(n-1)(n-2)}x_{j,n}$$

$$\beta_3 = \frac{1}{n}\sum_{j=4}^{n}\frac{(j-1)(j-2)(j-3)}{(n-1)(n-2)(n-3)}x_{j,n}$$

Then, t_2, t_3 and t_4, which are the estimations of the coefficient of variation (τ_2), L-skewness (τ_3) and L-kurtosis (τ_4), respectively, can be calculated as:

$$t_2 = L_2/L_1, t_3 = L_3/L_2, t_4 = L_4/L_2 \tag{8}$$

2.3.5 Return Period

The return period refers to the average time interval for rainfall that is greater than or equal to the intensity of a specific rainfall intensity within the statistical period and is the reciprocal of the frequency of the specific rainfall. It is the small probability problem on the right side of the probability distribution.

The extreme precipitation X_T under the return period of T years for the GEV, GP and gamma distributions can be calculated as follows:

For the GEV distribution: $X_T = \hat{\xi} + \frac{\hat{\alpha}}{\hat{k}}\left(1 - (-\ln(1 - 1/T))^{\hat{k}}\right)$

For the GP distribution: $X_T = \hat{\xi} + \frac{\hat{\alpha}}{\hat{k}}\left(1 - (1/T)^{\hat{k}}\right)$

where $\hat{\alpha}, \hat{\xi}$ and $\hat{k}$ are the estimates of α, ξ and k, respectively.

The quantiles of gamma distribution have no explicit analytical form and can be obtained by a numerical method, expressed as $X_T = F^{-1}(F(X_T))$.

2.3.6 Kolmogorov-Smirnov (K-S) Test

The K-S test was chosen to test goodness of fit to determine the best distribution for the extreme precipitation series in the HLR. The K-S test compares the empirical and theoretical frequency distributions of extreme precipitation

Table 1　The cumulative distribution functions (CDFs) and parameter estimations of GEV, GP and Gamma distributions

Distributions	CDF	Estimators of parameters
GEV	$F(x) = \exp\left\{-[1-(k(x-\xi))/\alpha]^{1/k}\right\}$ $k \neq 0$	$k \approx 7.8590z + 2.9554z^2$ $z = 2/(3+t_3) - \ln2/\ln3$ $\alpha = l_2 k / \left\{\left(1-2^{-k}\right)\Gamma(1+k)\right\}$ $\xi = l_1 - \alpha[1-\Gamma(1+k)]/k$
GP	$F(x) = 1-e^{-y}$ $y = -\ln[1-k(x-\xi)/\alpha]/k, k \neq 0$ $y - (x-\xi)/\alpha, k = 0$	$k = (1-3t_3)/(1+t_3)$ $\alpha = (1+k)(2+k)l_2$ $\xi = l_1 - (2+k)l_2$
Gamma	$f(x) = \frac{1}{\beta^\alpha \Gamma(\alpha)} \int_\xi^x x^{\alpha-1} e^{-x/\beta} dx$	$if\ 0 < t < 1/2, then z = \pi t_2^2$ $\alpha \approx \dfrac{1-0.3080z}{z-0.05812z^2 + 0.01765z^3}$ $if\ 1/2 < t < 1, then z = 1-t$ $\alpha \approx \dfrac{0.7213z - 0.5947z^2}{1-2.1817z + 1.2113z^2}$ $\beta = l_1/\alpha$

series. The test statistic is the maximum absolute difference (D_{max}) between the cumulative frequencies of empirical and theoretical frequencies. Under the significance level α, if D_{max} is calculated to be smaller than the critical value $D_\alpha(n)$ (n is sample size), then the probability model can be considered as a significantly fit model to the observed data. The probability distribution corresponding to the minimum value of D_{max} was selected as the optimal distribution.

3 Results and Discussion

3.1 The Spatial and Temporal Variation in Extreme Precipitation

The spatial distribution of mean values of the AM and POT series and the differences in mean and standard variance of AM and POT series are shown in Fig. 3, employing the inverse-distance weighted interpolation method to interpolate the values over the whole study area. The differences in the mean values of AM and POT series in almost all areas was positive, indicating that the mean values of the AM series were slightly higher than that of the POT series, which was the same result as that in Fig. 2. The results of hot spot analysis for spatial clustering of high and low values are shown in Fig.4. From Fig. 3 and Fig. 4, the AM and POT series showed similar spatial distribution. Hot spots under 90% and 95% confidence level were significant high value areas, and cold spots under 90% and 95% confidence level were significant low value areas. The high value area of extreme precipitation was located in the southeast part of the HLR, and the lower value area of the AM and POT series is mainly distributed in

the northwestern part of the HLR and the upper reaches of the Wuding River Basin.

The annual maximum precipitation series of all the stations during 1966–2015 were analyzed by the TFPW-MK method with a significance level of 0.05, and the results are shown in Fig. 5. Up and down arrows indicate increasing trends and decreasing trends, respectively. The larger size of the arrows represents a significant change trend with a significance level of 0.05. It can be seen that the maximum precipitation of 60 stations had decreasing trends during 1966–2015, and there were 60 stations showing increasing trends. Only two stations showed significant increasing trends, including Kaifu and Yanchuan, which are located in the middle and southern part of the HLR, respectively, and the changing trends of the remaining stations were nonsignificant under the 95% confidence level.

3.2 The Best Distributions for Extreme Precipitation

In this study, the GEV, GP and gamma distributions were used to fit the distributions of the AM and POT series in the HLR from 1966 to 2015. The parameters of each used distribution were estimated by L-moments method, and the optimal model was selected for each station by the K-S test under 95% confidence level. Figure 6 and Table 2 show the results of K-S test and the best distribution of selected stations.

From Fig. 6a and Table 2, it can be seen that there were 96 stations that could be better fitted by the GEV distribution for the AM series, while there were only 11 stations and 13 stations that could be better fitted by the GP and gamma distributions for the AM series, respectively. It was also found that the GEV and gamma distributions had passed the K-S test
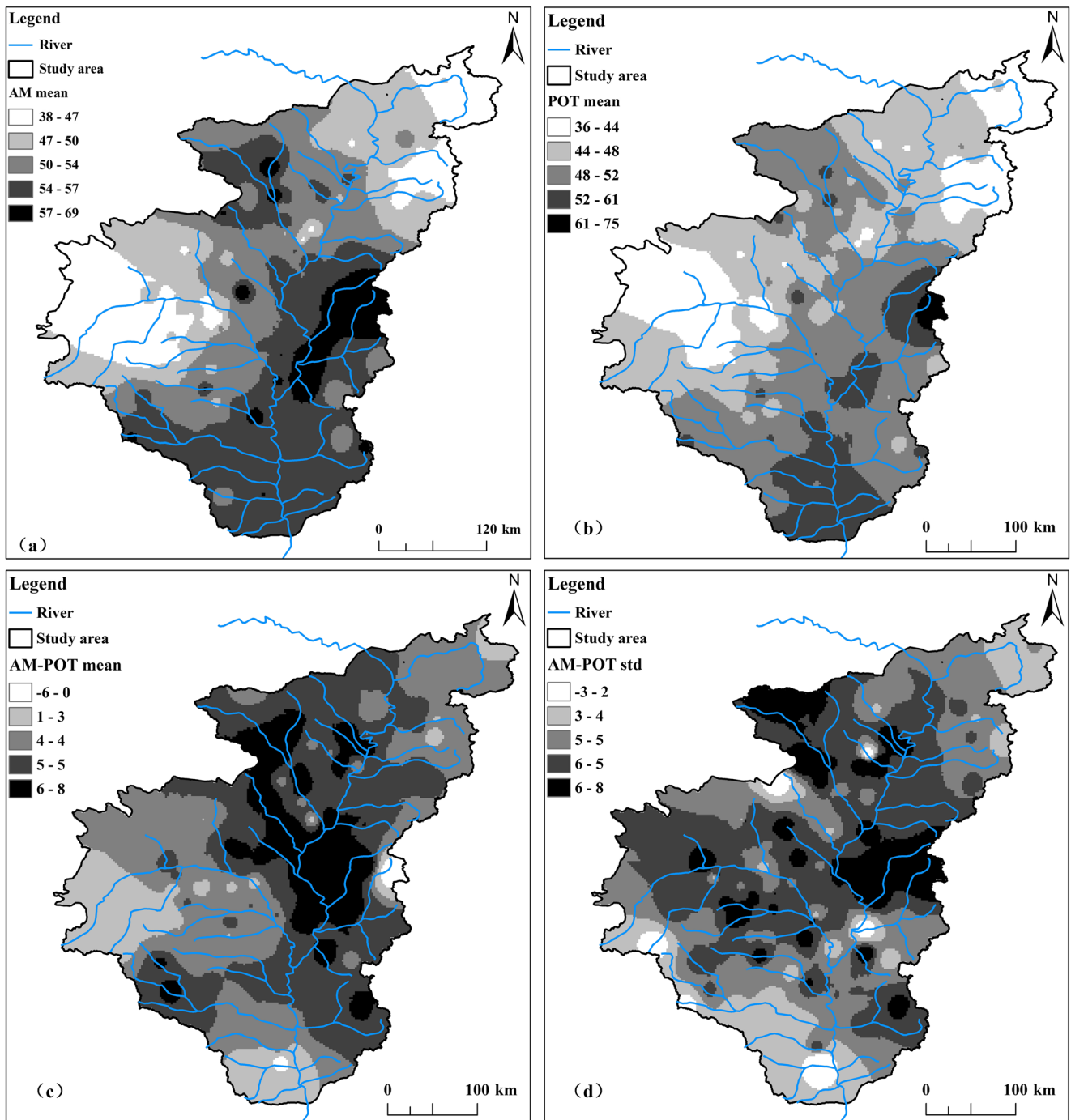
Fig. 3 Spatial distributions of mean of (**a**) AM series and (**b**) POT series and differences in (**c**) mean and (**d**) standard variance of AM and POT series in the HLR (unit: mm)

under the 95% confidence level for all of the 120 selected stations, while the GP distribution had not passed the K-S test under the 95% confidence level for 16 stations. Therefore, the GEV distribution can better fit the AM series in the HLR, and it can be inferred that the AM series was not suitable for simulation with the GP distribution in the HLR compared to the GEV and gamma distributions.

From Fig. 6 and Table 2, there were 94 stations best fitted by the GP distribution and 26 stations best fitted by the GEV distribution for the POT series, while no station could be better fitted by the gamma distribution for the POT series. All of these distributions have passed the K-S test under the 95% confidence level. It was found that the GEV distribution can better fit the AM series, and the GP distribution can better fit the POT series.
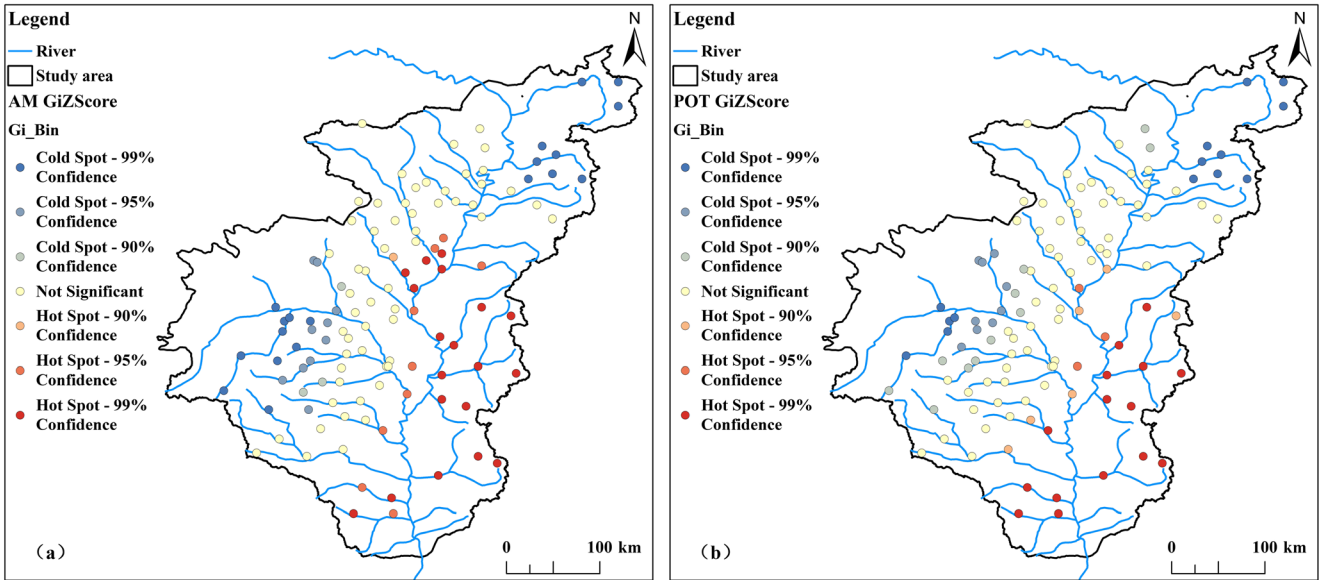
Korean Meteorological Society 🍃 Springer

Fig. 4 Spatial distribution of hot spot analysis results of (**a**) AM and (**b**) POT series in the HLR

Figure 7 shows the empirical and theoretical cumulative distributions fitted for the AM and POT series with the GEV, GP and gamma distributions at the Suide precipitation station. It can be seen that the GEV distribution can better simulate the variation in extreme precipitation both in the tail and in the middle part for the AM series. Similarly, the GP distribution can better simulate the POT series.

Unqualified represents the model has not passed the KS test under the 95% confidence level.

Fig. 5 The changing trends of the AM series in the HLR during 1966–2015. The 0.05 significant level is considered
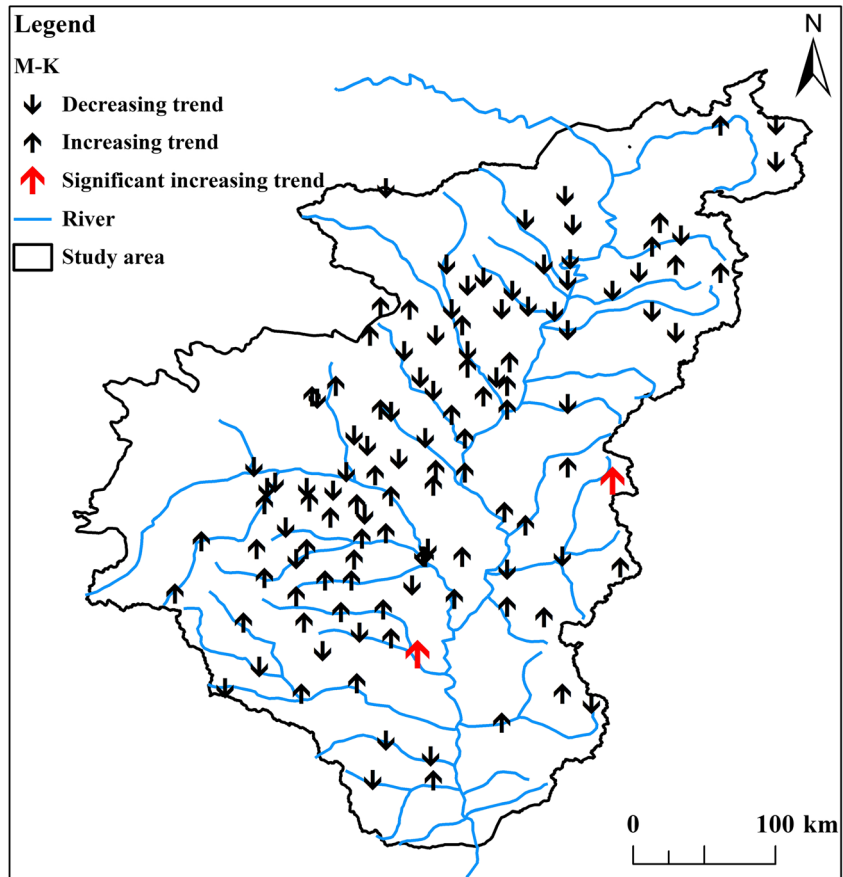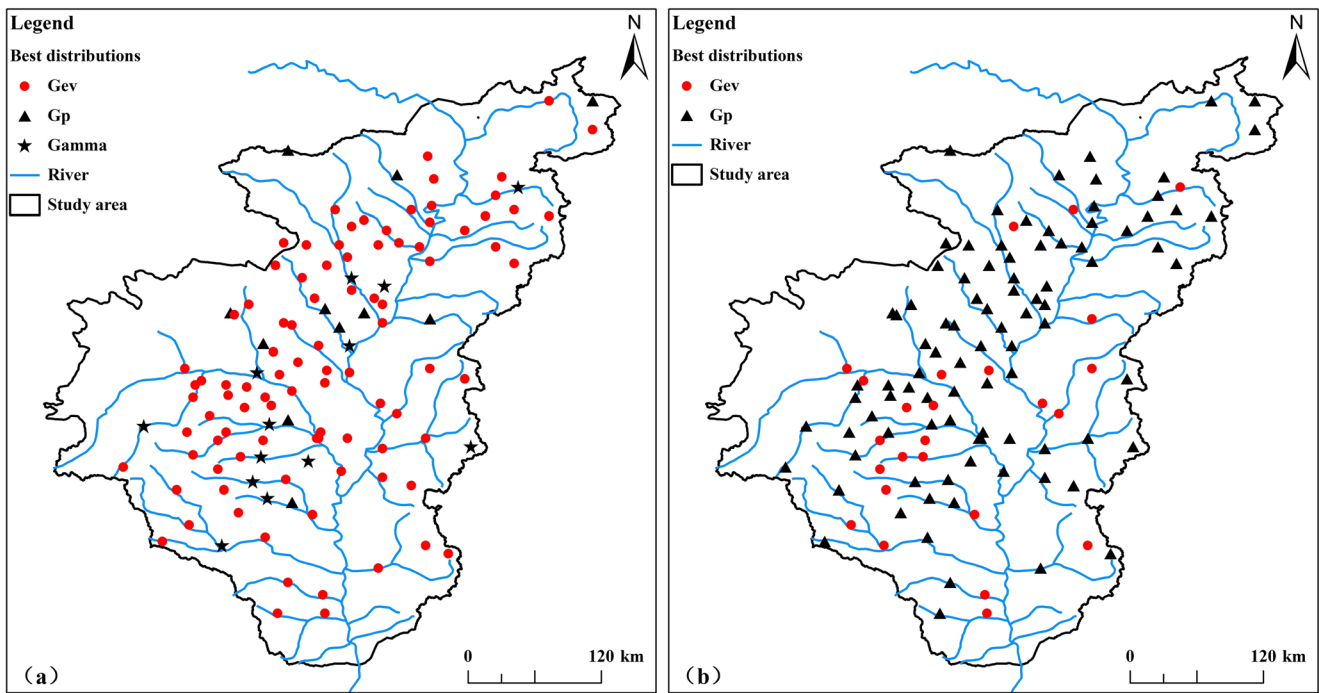
Fig. 6 Best distributions for (**a**) AM and (**b**) POT series according to the K-S test for all stations in the HLR (The red circle, black triangle and black pentagrams indicate that the optimal distribution for the station are the GEV, GP and gamma distributions, respectively)

Table 2 The numbers of stations that passed and failed the K-S test and best distributions for the AM and POT series

Series		GEV		GP		Gamma	
		Passed	Unqualified	Passed	Unqualified	Passed	Unqualified
AM		120	0	106	14	120	0
POT		120	0	120	0	120	0
Best distribution	AM	96	–	11	–	13	–
	POT	26	–	94	–	0	–

3.3 Estimated Extreme Precipitation under Different Return Periods

According to the best fit distribution results given in Fig. 6, the extreme precipitation of the AM and POT series in each station under return periods of 5, 10, 25 and 50 years was calculated, as shown in Figs. 8 and 9.

For the AM series, the spatial variations in extreme precipitation were similar under different return periods (Fig. 8). The maximum values were concentrated in the

Fig. 7 Empirical and theoretical cumulative distributions fitted for (**a**) AM and (**b**) POT series at the Suide station
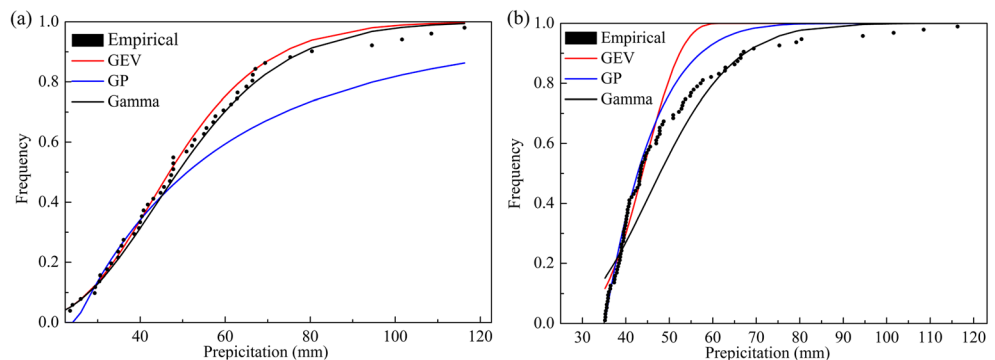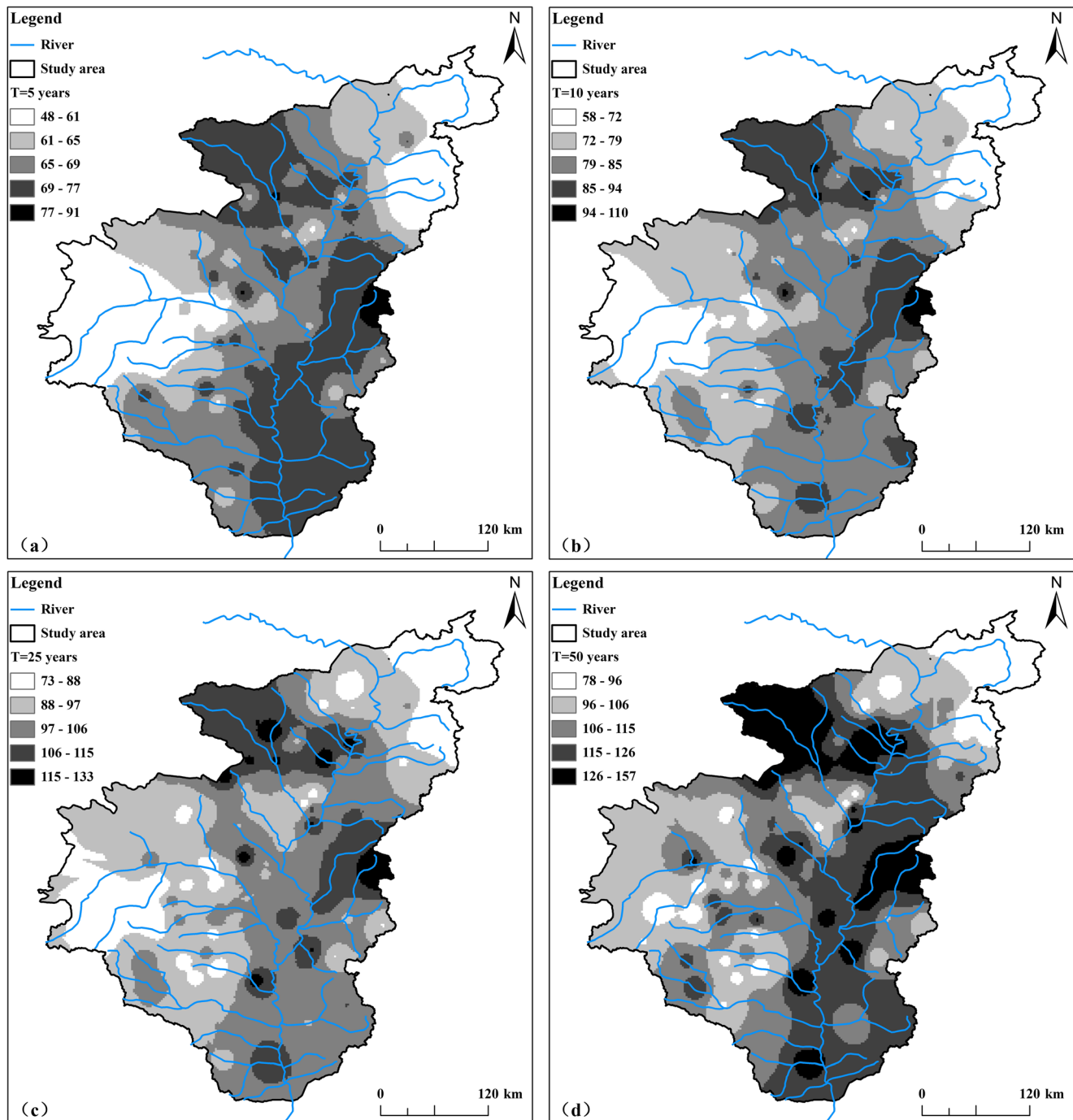
Fig. 8 Spatial distribution of estimated extreme precipitation under different return periods: (**a**) 5, (**b**) 10, (**c**) 25, and (**d**) 50 years of the AM series in the HLR (unit: mm)

upper reaches of the Kuye River basin, Qiushui River basin and the southern part of the HLR, which is similar to the multiyear average distribution of the AM series in Fig. 3. As shown in Fig. 9, the spatial variation in extreme precipitation of the POT series under a return period of 50 years is similar to that of the AM series, while the

maximum values under return periods of 5, 10 and 25 years were concentrated in the upper reaches of the Kuye River and Qiushui River Basins, as well as the southern part of the HLR, which covered a slightly smaller area compared to those of the AM series. The estimated extreme precipitation of the POT series was a slightly
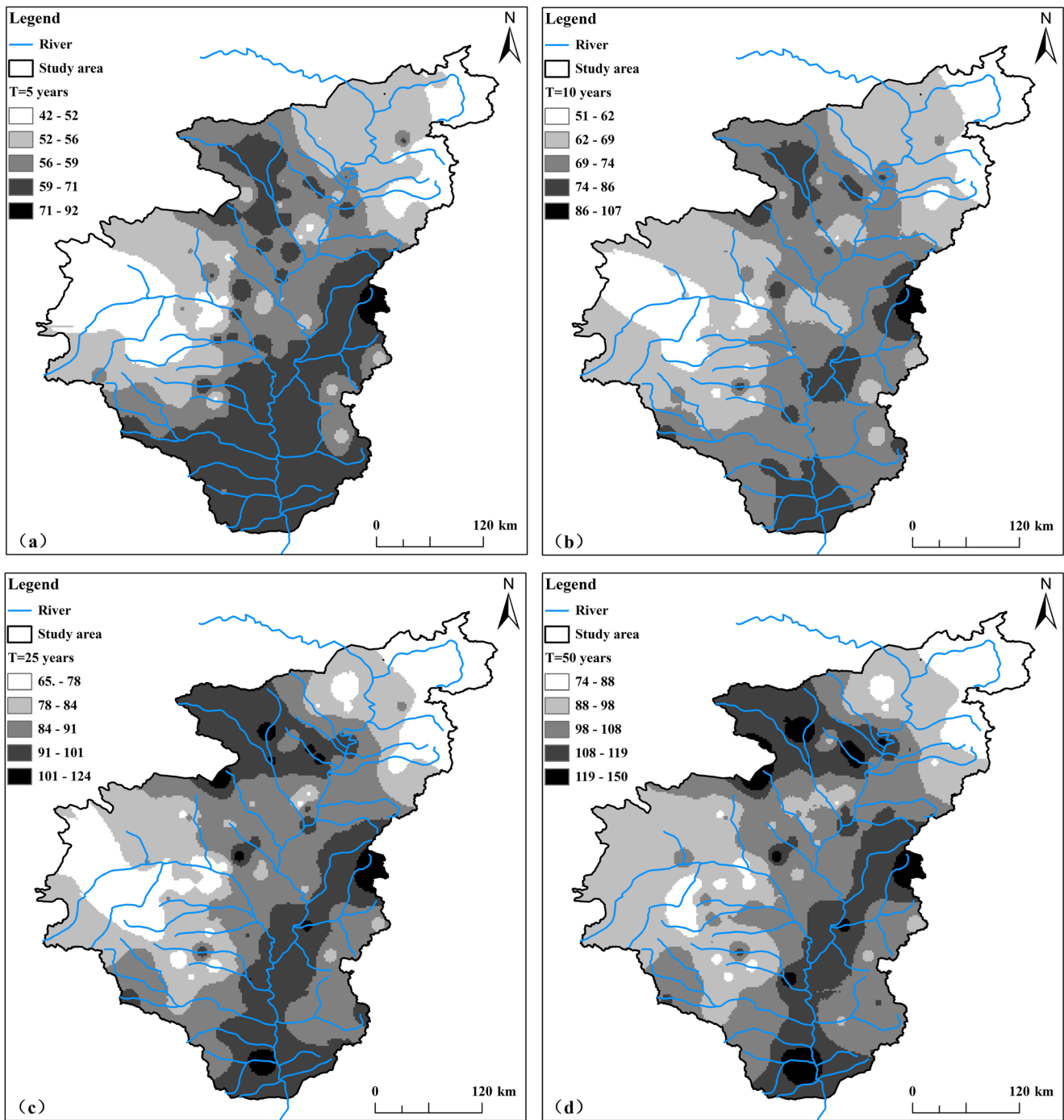
Fig. 9 Spatial distribution of estimated extreme precipitation under different return periods: (**a**) 5, (**b**) 10, (**c**) 25, and (**d**) 50 years of the POT series in the HLR (unit: mm)

smaller than that of the AM series with the same return period at most stations (Figs. 8 and 9).

Figure 10 shows the comparisons of observed and estimated precipitation by the GEV, GP and gamma distributions of the AM and POT series with a return period from 1 to 100 years at the Suide station. It can be found that the estimated precipitation by the GEV distribution

and GP distribution can better fit the observed precipitation of the AM series and POT series, respectively. This result is the same as that of the K-S test; on the other hand, this result indicates that the GEV and GP distributions can better fit the AM and POT series, respectively.

By comparing the estimated extreme precipitation under a return period of 50 years and the corresponding observed

Korean Meteorological Society 🌐 Springer

Fig. 10 Comparisons of observed and predicted precipitation by different distributions for AM and POT series at the Suide station
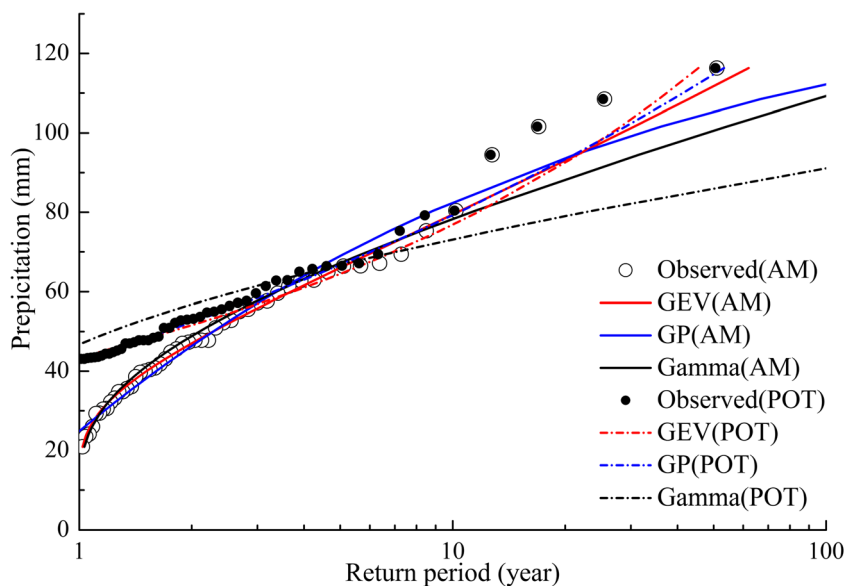

values as shown in Figs. 8d, 9d and 11, the spatial distribution of the estimated extreme precipitation values of the AM and POT series were similar to the observed values, while the estimated extreme precipitation of the AM and POT series were smaller than the observed precipitation.

From the comparison of the spatial distribution of maximum precipitation and relative errors between observed and estimated extreme precipitation with the optimal distribution under a return period of 50 years (Figs. 11 and 12), the stations with relatively high relative errors were distributed in areas with high precipitation. There is great uncertainty in the occurrence of extreme precipitation events, and the prediction of extreme precipitation still needs further exploration.

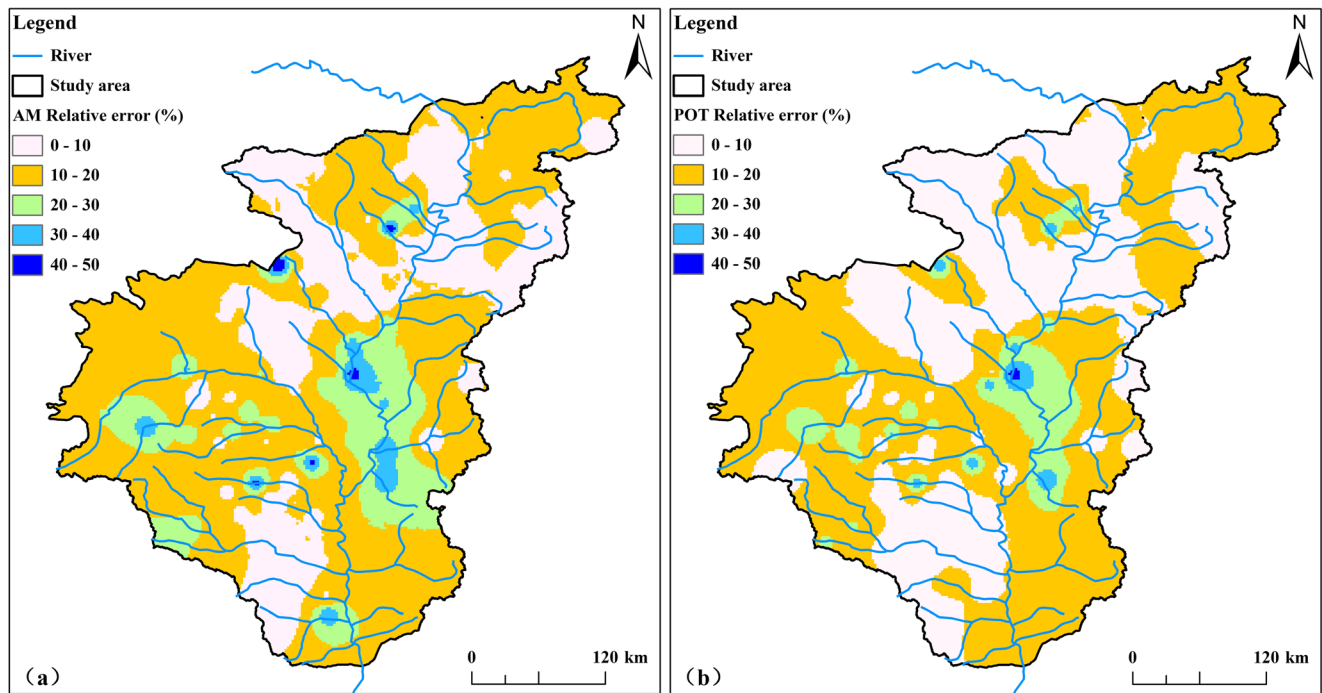**Fig. 11** Spatial distribution of maximum precipitation during 1966–2015 (unit: mm)
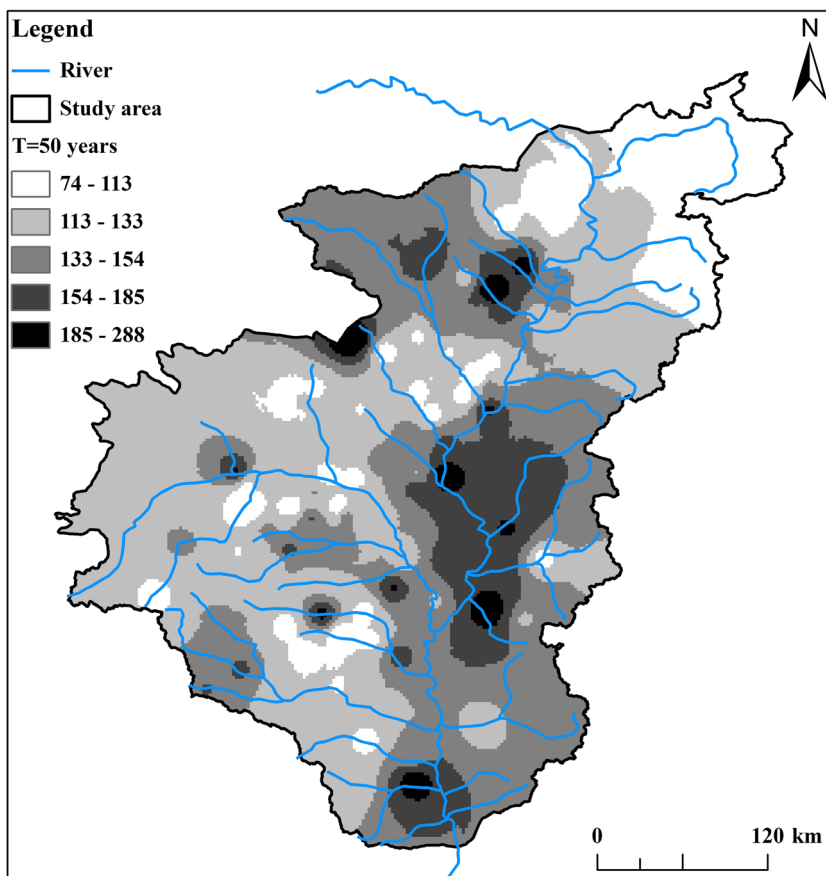
Fig. 12 Spatial distributions of relative errors between observed and estimated extreme precipitation under a return period of 50 years with the optimal distribution of (**a**) AM and (**b**) POT series

4 Conclusions

In this research, the AM and POT series of extreme precipitation were selected based on the daily precipitation data of 9 meteorological stations and 111 precipitation stations in the HLR of the Yellow River basin during 1966–2015 to analyze the spatial-temporal variations in and statistical probability characteristics of extreme precipitation. The main conclusions are given as follows:

(1) High value area of extreme precipitation were located in the southeast part of the HLR, and the lower value area of the AM and POT series is mainly distributed in the northwestern part of the HLR and the upper reaches of the Wuding River Basin.

(2) In the past 50 years, extreme precipitation at half of the selected stations showed a decreasing trend, and extreme precipitation at the other half of the stations showed an increasing trend. At the significance level of 0.05, only two stations showed significant increasing trends in extreme precipitation, and the changing trends of extreme precipitation at the remaining stations were not significant.

(3) With the application of the GEV, GP and gamma distributions and K-S test, the GEV distribution can better fit the AM series, while the GP distribution can better fit the POT series. The estimated extreme precipitation of the AM series was larger than that of POT series with the same return period at most stations. The spatial

distributions of the estimated extreme precipitation of AM and POT series by the optimal distribution with a return of 50 years were similar to the observed values, but the values were smaller than the observed ones.

Compliance with Ethical Standards

Competing Interests   The authors declare that they have no competing interests.

References

Aguilar, E., Barry, A.A., Brunet, M., Ekang, L., Fernandes, A., Massoukina, M., et al.: Changes in temperature and precipitation extremes in western Central Africa, Guinea Conakry, and Zimbabwe, 1955–2006. J. Geophys. Res. Atmos. **114**(D2), 356–360 (2009)

Alexander, L.V., Zhang, X., Peterson, T.C., et al.: Global observed changes in daily climate extremes of temperature and precipitation. J. Geophys. Res.-Atmos. **111**(D5), 1042–1063 (2006)

Bayazit, M., Önöz, B.: To prewhiten or not to prewhiten in trend analysis? Hydrol. Sci. J. **52**(4), 611–624 (2007)

Cai, J., Jiang, Z.: Advantages of L-moment estimation and its application to extreme precipitation. Acta Meteorol. Sin. **20**, 248–260 (2007) (in Chinese)

Chen, Y., Zhang, Q., Xiao, M., Singh, V., Leung, Y., Jiang, L.: Precipitation extremes in the Yangtze River basin, China: regional frequency and spatial-temporal patterns. Theor Appl Climatol. **116**(3–4), 447–461 (2014)

Chen, Y.Z., Guan, Y.Q., Shao, G.W., Zhang, D.R.: Investigating trends in streamflow and precipitation in Huangfuchuan Basin with wavelet analysis and the Mann-Kendall test. Water. **8**(3), 77 (2016)

Du, H., Xia, J., Zeng, S., She, D., Liu, J.: Variations and statistical probability characteristic analysis of extreme precipitation events under climate change in Haihe River basin, China. Hydrol. Process. **28**(3), 913–925 (2014)

Easterling, D.R., Meehl, G.A., Parmesan, C., et al.: Climate extremes: observations, modeling, and impacts. Science. **289**(5487), 2068–2074 (2000)

Fiddes, S.L., Pezza, A.B.: Current and future climate variability associated with wintertime precipitation in alpine Australia. Clim. Dyn. **44**(9–10), 2571–2587 (2014)

Fiddes, S.L., Pezza, A.B., Barras, V.: Synoptic climatology of extreme precipitation in alpine Australia. Int. J. Climatol. **35**(2), 172–188 (2015)

Fischer, T., Su, B., Luo, Y., Scholten, T.: Probability distribution of precipitation extremes for weather index-based insurance in the Zhujiang River basin, South China. J. Hydrometeorol. **13**(3), 1023–1037 (2011)

Frich, P., Alexander, L.V., DellaMarta, P., et al.: Observed coherent changes in climatic extremes during the second half of the twentieth century. Clim. Res. **19**(3), 193–212 (2002)

Gao, Y., Feng, Q., Liu, W., Lu, A., Wang, Y., Yang, J., et al.: Changes of daily climate extremes in loess plateau during 1960–2013. Quat. Int. **371**(1), 5–21 (2015)

Groisman, P.Y., Karl, T.R., Easterling, D.R., et al.: Changes in the probability of heavy precipitation: important indicators of climatic change. Clim. Chang. **42**(1), 243–283 (1999)

Hosking, J.R.M.: L-moments analysis and estimation of distributions using linear combination of order statistics. J. R. Stat. Soc. **52**(1), 105–124 (1990)

Hosking, J. R. M., & Wallis, J. R. Regional Frequency Analysis. Cambridge University Press (1997)

Hu, C., Chen, X., Chen, J.: Spatial distribution and its variation process of sedimentation in Yellow River. J. Hydraul. Eng. **39**(5), 10–19 (2008). (in Chinese)

Hu, Z., Li, Q., Chen, X., et al.: Climate changes in temperature and precipitation extremes in an alpine grassland of Central Asia. Theor Appl Climatol. **56**(4), 1–13 (2015)

IPCC. Summary for policymakers. In Climate Change 2013: the physical science basis. Contribution of Working Group I to the Fifth Assessment Report of the Intergovernmental Panel on Climate Change, Stocker, T., Qin, D., Plattner, G., Tignor, M., Allen, S., Boschung, J., Nauels, A., Xia, Y., Bex, V., Midgley, P. (eds). Cambridge University Press: Cambridge, UK and New York, NY (2013)

Jiang, Z., Shen, Y., Ma, T., Zhai, P., Fang, S.: Changes of precipitation intensity spectra in different regions of mainland China during 1961–2006. J. Meteorol. Res. **28**(6), 1085–1098 (2014)

Kendall, M.G.: Rank Correlation Methods. Griffin, London (1955)

Kioutsioukis, I., Melas, D., Zerefos, C.: Statistical assessment of changes in climate extremes over Greece (1955–2002). Int. J. Climatol. **30**(11), 1723–1737 (2010)

Li, Z., Zheng, F.L., Liu, W.Z., Flanagan, D.C.: Spatial distribution and temporal trends of extreme temperature and precipitation events on the loess plateau of China during 1961–2007. Quat. Int. **226**(1), 92–100 (2010)

Liang, L., Zhao, L., Gong, Y., Tian, F., Wang, Z.: Probability distribution of summer daily precipitation in the Huaihe Basin of China based on gamma distribution. Acta Meteorol. Sin. **26**(1), 72–84 (2012)

Limsakul, A., Singhruck, P.: Long-term trends and variability of total and extreme precipitation in Thailand. Atmos. Res. **169**, 301–317 (2016)

Liu, C., Xia, J.: Water problems and hydrological research in the Yellow River and the Huai and Hai River basins of China. Hydrol. Process. **18**(12), 2197–2210 (2004)

Mann, H.B.: Nonparametric tests against trend. Econometrica. **13**, 245–259 (1945)

Mirza, M.M.Q.: Climate change and extreme weather events: can developing countries adapt? Clim. Pol. **3**(3), 233–248 (2003)

Mitchell, J.M., Dzerdzeevskii, B., Flohn, H.: Climate Change. WHO Technical Note 79 World Meteorological Organization, p. 79, Geneva (1966)

Plummer, N., Salinger, M.J., Nicholls, N., et al.: Changes in climate extremes over the Australian region and New Zealand during the twentieth century. Clim. Chang. **42**(1), 183–202 (1999)

Ran, D.: Review on the variation of water and sediment in the he-long reach in the middle reaches of the Yellow River. J. Sediment. Res. (3), 72–81 (2000) (in Chinese)

Saifullah, M., Li, Z., Li, Q., et al.: Quantitative estimation of the impact of precipitation and land surface change on hydrological processes through statistical modeling. Adv. Meteorol. (1), 1–15 (2016)

Santos, M., Fragoso, M.: Precipitation variability in northern Portugal: data homogeneity assessment and trends in extreme precipitation indices. Atmos. Res. **131**(5), 34–45 (2013)

Sen Roy, S., Balling, R.C.: Trends in extreme daily precipitation indices in India. Int. J. Climatol. **24**(4), 457–466 (2004)

She, D., Xia, J., Song, J.: Spatio-temporal variation and statistical characteristic of extreme dry spell in Yellow River Basin, China. Theor. Appl. Climatol. **112**(1–2), 201–213 (2013)

She, D., Shao, Q., Xia, J., Taylor, J.A., Zhang, Y., Zhang, L., et al.: Investigating the variation and non-stationarity in precipitation extremes based on the concept of event-based extreme precipitation. J. Hydrol. **530**, 785–798 (2015a)

She, D., Xia, J., Zhang, D., Ye, A., Sood, A.: Regional extreme-dry-spell frequency analysis using the L-moments method in the middle reaches of the Yellow River basin. China. Hydrol. Process. **28**(17), 4694–4707 (2015b)

Su, B., Jiang, T., Dong, W.: Probabilistic characteristics of precipitation extremes over the Yangtze River basin. Scientia Meteor. Sinica. **28**(6), 625–629 (2008). (in Chinese)

Su, B., Kundzewicz, Z.W., Jiang, T.: Simulation of extreme precipitation over the Yangtze River basin using Wakeby distribution. Theor Appl Climatol. **96**(3–4), 209–219 (2009)

Sun, Q., Miao, C., Duan, Q., Wang, Y.: Temperature and precipitation changes over the loess plateau between 1961 and 2011, based on high-density gauge observations. Glob. Planet. Chang. **132**(1), 1–10 (2015)

Sun, W., Mu, X., Song, X., Wu, D., Cheng, A., Qiu, B.: Changes in extreme temperature and precipitation events in the loess plateau (China) during 1960–2013 under global warming. Atmos. Res. **168**(22), 33–48 (2016)

Wan, L., Zhang, X.P., Ma, Q., Zhang, J.J., Ma, T.Y., Sun, Y.P.: Spatiotemporal characteristics of precipitation and extreme events on the loess plateau of China between 1957 and 2009. Hydrol. Process. **28**(18), 4971–4983 (2015)

Wang G. Yellow River Flood. Zhengzhou: the Yellow River Water Conservancy Press, 103–114 (1997). (in Chinese)

Wang, Z., Qian, Y.: Frequency and intensity of extreme precipitation events in China. Adv. Water Sci. **20**, 1–9 (2009) (in Chinese)

Wang, Q.X., Wang, M.B., Fan, X.H., Zhang, F., Zhu, S.Z., Zhao, T.L.: Trends of temperature and precipitation extremes in the loess plateau region of China, 1961–2010. Glob. Planet. Chang. **129**(3–4), 949–963 (2017)

Wijngaard, J.B., Tank, A.M.G.K., Konnen, G.P.: Homogeneity of 20th century european daily temperature and precipitation series. Int. J. Climatol. **23**(6), 679–692 (2003)

Xia, J., She, D., Zhang, Y., et al.: Spatio-temporal trend and statistical distribution of extreme precipitation events in Huaihe River basin during 1960-2009. J. Geogr. Sci. **22**(2), 195–208 (2012)

Xia, J., Peng, S., Wang, C., Hong, S., Chen, J., Luo, X.: Impact of climate change on water resources and adaptive management in the Yellow River Basin. Yellow River. **36**(10), 1–4 (2014) (in Chinese)

Xiong, L., Guo, S.: Application of L-moments in the regional flood frequency analysis. Water Power. **29**(3), 6–8 (2003). (in Chinese)

You, Q., Kang, S., Aguilar, E., Pepin, N., Flügel, W.A., Yan, Y., et al.: Changes in daily climate extremes in China and its connection to the large scale atmospheric circulation during 1961–2003. Clim. Dyn. **36**(11–12), 2399–2417 (2011)

Yue, S. and Wang, C.Y. The Applicability of pre-whitening to eliminate the influence of serial correlation on the Mann-Kendall test. Water Resour. Res., 38, 4-1–4-7 (2002)

Zhai, P., Zhang, X., Wan, H., Pan, X.: Trends in total precipitation and frequency of daily precipitation extremes over China. J. Clim. **18**(18), 1096–1108 (2005)

Zhang, Q., Peng, J., Singh, V.P., Li, J., Chen, Y.D.: Spatio-temporal variations of precipitation in arid and semiarid regions of China: the Yellow River Basin as a case study. Glob. Planet. Chang. **114**(2), 38–49 (2014)

Zhang, Y., Xia, J., She, D.: Spatiotemporal variation and statistical characteristic of extreme precipitation in the middle reaches of the Yellow River Basin during 1960–2013. Theor Appl Climatol. **15**, 1–18 (2018)

Zheng, H., Lu, Z., Zhu, R., et al.: Responses of streamflow to climate and land surface change in the headwaters of the Yellow River Basin. Water Resour. Res. **45**(7), 641–648 (2009)